Supporting Information

Experimentally validated hERG pharmacophore models as cardiotoxicity prediction tools

Jadel M. Kratz,[†,§] Daniela Schuster,[,‖] Michael Edtbauer,[‖] Priyanka Saxena,[⊥] Christina E. Mair,[§] Julia Kirchebner,[‖] Barbara Matuszczak,[‖] Igor Baburin,[⊥] Steffen Hering,[⊥] Judith M. Rollinger[*,§]*

[†] Departamento de Ciências Farmacêuticas, Universidade Federal de Santa Catarina, 88.040-900, Florianópolis, SC, Brazil.

[§] Institute of Pharmacy/Pharmacognosy and Center for Molecular Biosciences Innsbruck, University of Innsbruck, Innrain 80-82, 6020 Innsbruck, Austria.

[‖] Institute of Pharmacy/Pharmaceutical Chemistry and Center for Molecular Biosciences Innsbruck, University of Innsbruck, Innrain 80-82, 6020 Innsbruck, Austria.

[⊥] Department of Pharmacology and Toxicology, University of Vienna, Althanstraße 14, 1090 Vienna; Austria.

* corresponding authors

Daniela Schuster - Daniela.Schuster@uibk.ac.at

Judith M. Rollinger – Judith.Rollinger@uibk.ac.at

Table of contents:

Table S1. Training set screening results with the Catalyst model.

Compound	Experimental IC_{50} [µM]	Found by Model
3	0.0067	x
4	0.0147	x
6	0.0181	x
7	0.0268	x
8	0.0332	x
9	0.0546	x
10	0.125	x
11	0.148	x
1	0.213	x
12	0.2313	x
13	0.32	x
14	0.32	x
15	3.2	
16	4.49	x
17	11.6	
18	14.2	x
19	133.3	
20	244.8	

All IC_{50} values were retrieved from Ekins et al., 2002.[1]

Chart S1. All 50 compounds selected for hERG block screening. Compounds were tested at 30 μM and were considered active, if ≥ 30% reduction of the peak tail hERG current was achieved.

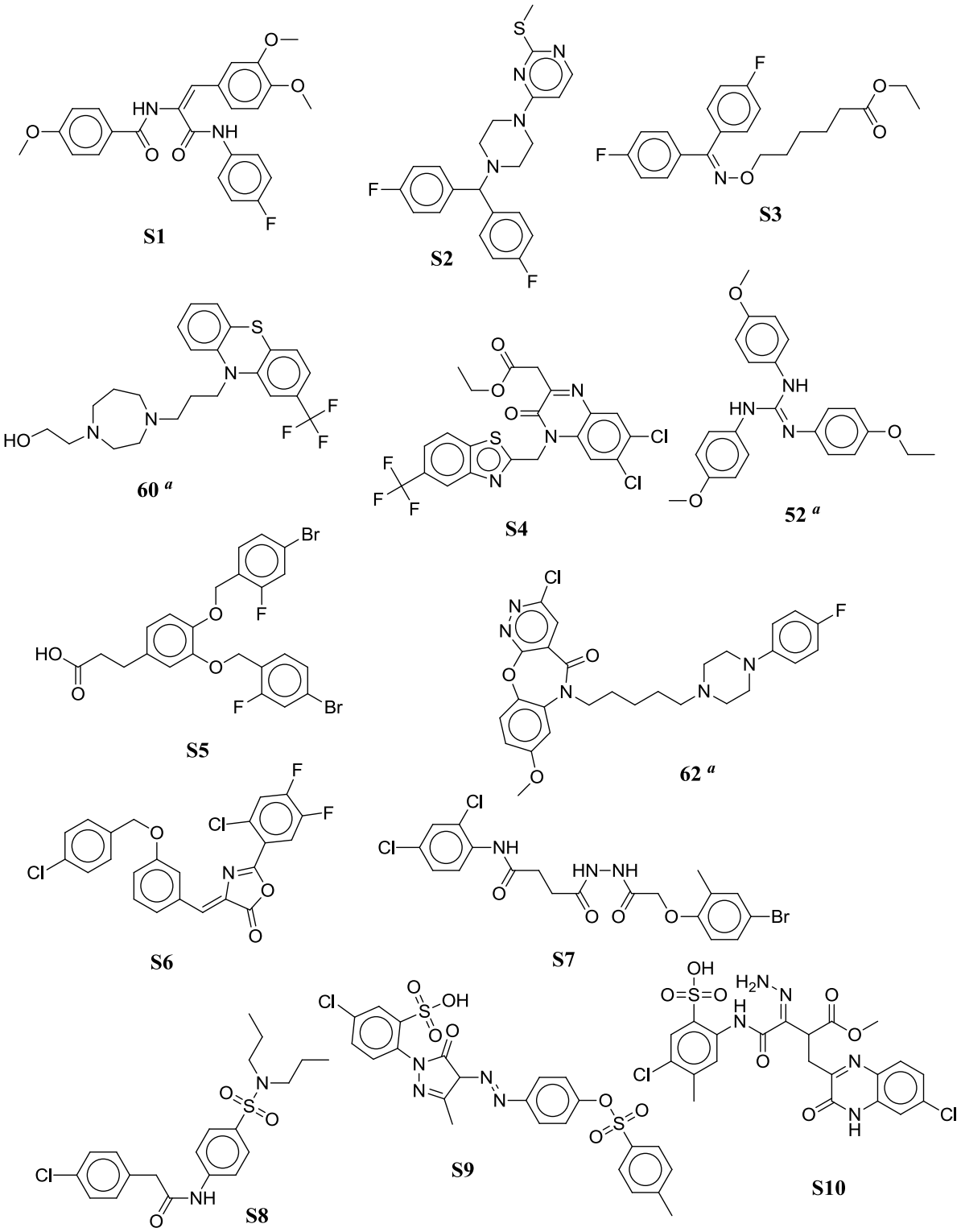

[a] Active compound (≥ 30% hERG inhibition)

Chart S1. … continued.

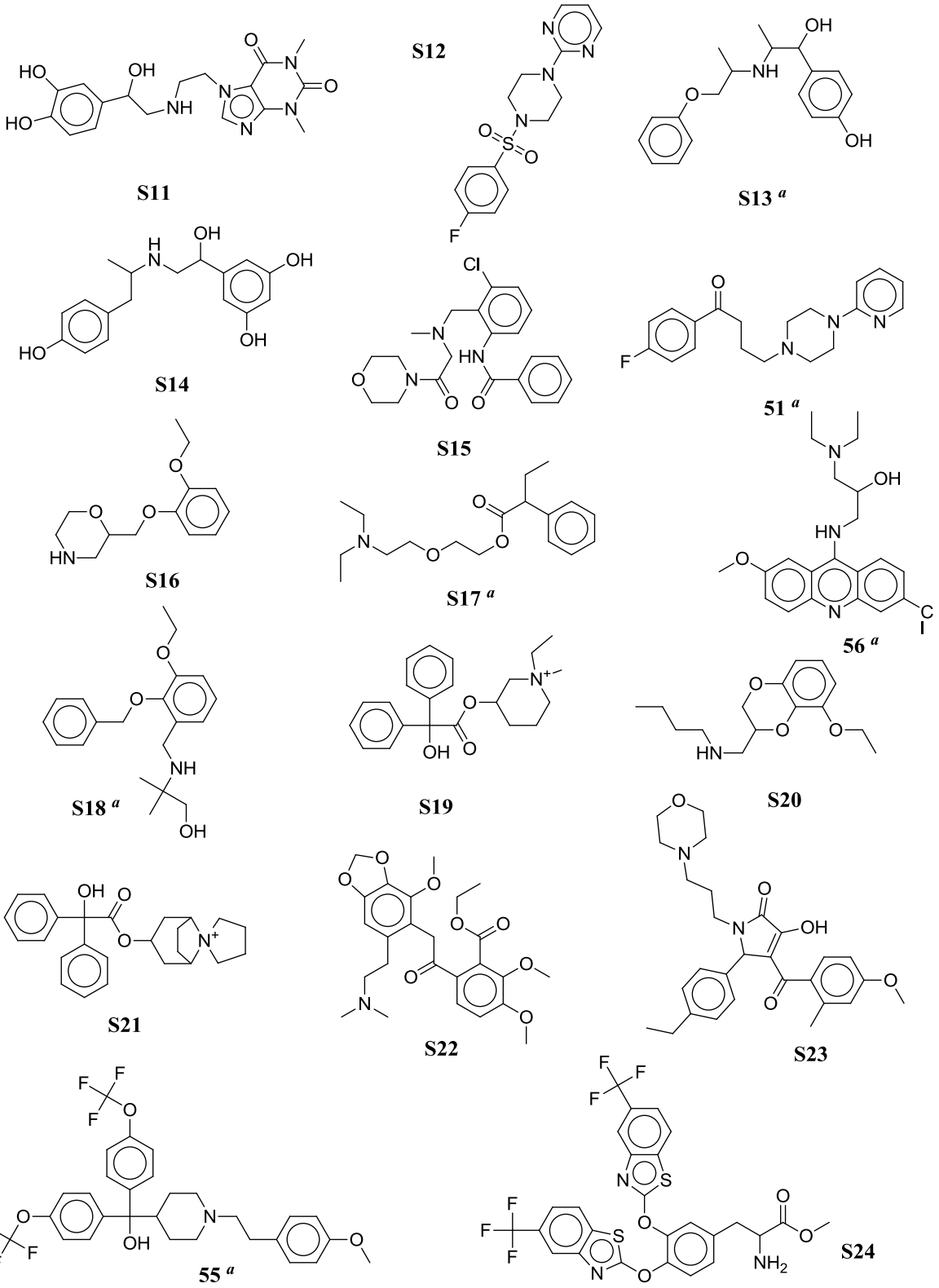

[a] Active compound (≥ 30% hERG inhibition)

Chart S1. … continued.

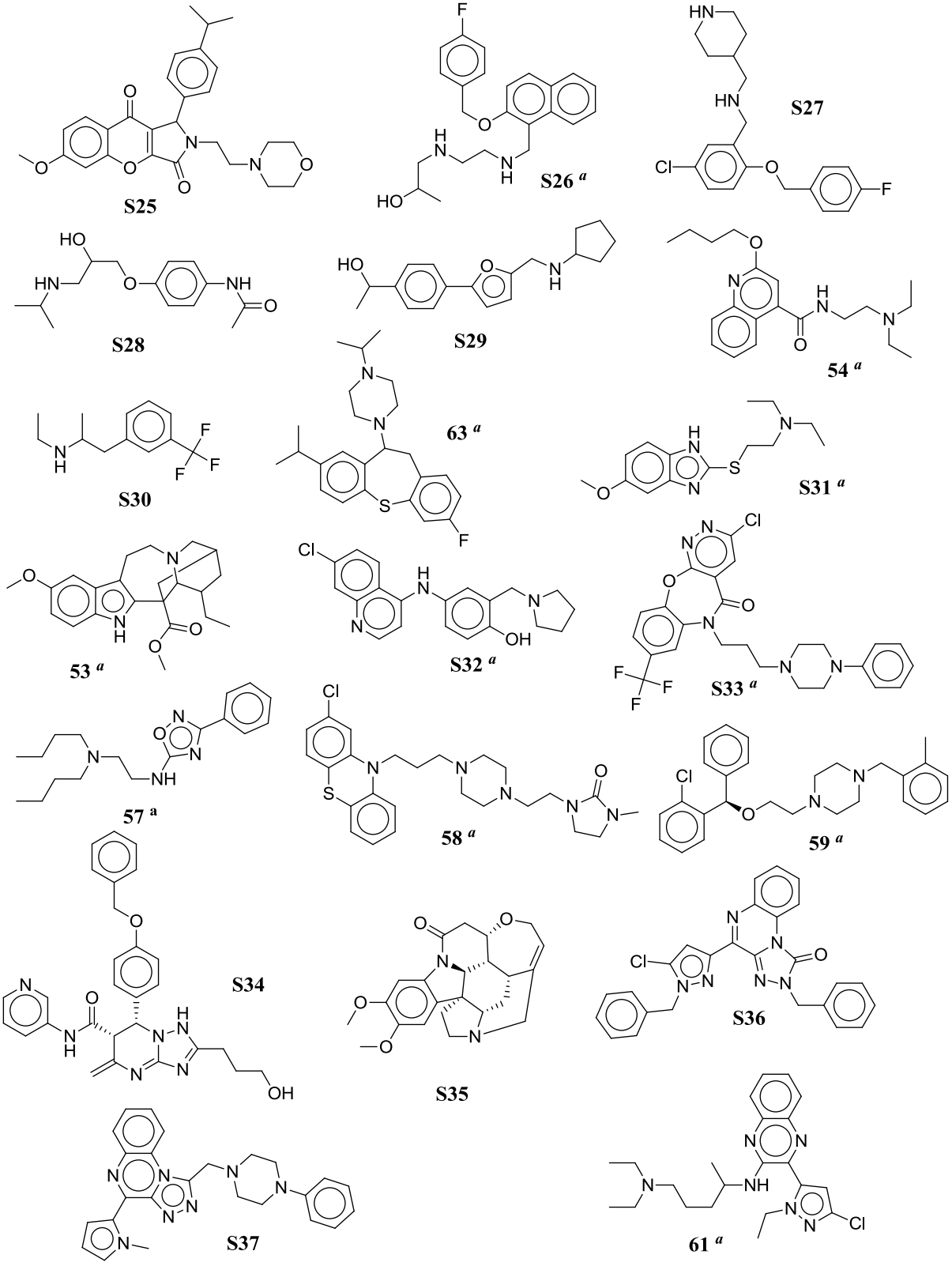

[a] Active compound (≥ 30% hERG inhibition)

Table S2. Fit-scores, pharmacophores overlapping and complete screening information.

	Compound	Model[a]	Fit-score[b]	Overlap[c]	Source[d]	Inhibition (%)[e]	
						Mean	SE
1	**S1**	M1	58.22		SPECS SP	13.22	0.42
2	**S2**	M1	57.82		SPECS SP	2.98	1.10
3	**S3**	M1	57.70		In-house	0.97	0.18
4	**60**	M1	56.65	M6	In-house	72.12	6.57
5	**S4**	M1	56.00		In-house	2.50	1.59
6	**52**	M1	55.66		In-house	54.63	5.64
7	**S5**	M1	55.49		In-house	4.26	0.39
8	**62**	M1	55.48	Catalyst	In-house	69.43	1.19
9	**S6**	M2	58.07		SPECS SP	4.15	2.67
10	**S7**	M2	58.02		SPECS SP	5.09	2.38
11	**S8**	M2	56.93		SPECS SP	8.16	0.41
12	**S9**	M2	56.91		In-house	1.18	0.64
13	**S10**	M2	55.99		In-house	3.21	0.06
14	**S11**	M3	57.42		In-house	3.46	1.69
15	**S12**	M3	57.08		In-house	9.63	5.13
16	**S13**	M3	56.35		In-house	34.97	3.32
17	**S14**	M3	56.27		In-house	6.15	3.65
18	**S15**	M3	56.08		In-house	14.36	1.14
19	**51**	M3	56.01		In-house	56.13	9.87
20	**S16**	M4	56.70		In-house	8.03	2.09
21	**S17**	M4	56.63		In-house	32.34	5.87
22	**56**	M4	56.43	Catalyst	In-house	51.61	9.47
23	**S18**	M4	56.40	Catalyst	In-house	32.79	1.46
24	**S19**	M4	56.40		In-house	6.95	0.02
25	**S20**	M4	56.39		In-house	18.73	4.17
26	**S21**	M4	56.07		In-house	2.93	0.99
27	**S22**	M4	55.82		In-house	21.96	1.12
28	**S23**	M5	56.88		SPECS SP	1.25	0.77
29	**55**	M5	56.79		SPECS SP	66.14	9.49

[a]Predicted hit selected for biological screening to validate this specific model (compounds were selected to cover all pharmacophore models developed in this study). [b]Fit-score generated with the "pharmacophore-fit" scoring function in LigandScout. It is a quantitative metric that indicates how well the chemical functions of the ligand geometrically map the features of the pharmacophore model. [c]Some compounds are consensus hits of different models. This column describes the overlapping of positive hits. [d]Source from where the compound was obtained. [e]Percentage of peak tail hERG current reduction obtained at a compound's concentration of 30 µM in the oocyte assay ($n \geq 3$). hERG inhibition classification is color-coded: red – inactive (inhibition < 30%); light green – active with inhibition between 30 and 50%; dark green – active with inhibition ≥ 50% (compounds selected for IC_{50} determination).

Table S2. … continued.

	Compound	Model[a]	Fit-score[b]	Overlap[c]	Source[d]	Inhibition (%)[e]	
						Mean	SE
30	**S24**	M5	55.58	Catalyst	In-house	14.30	7.73
31	**S25**	M5	55.50		SPECS SP	15.30	1.84
32	**S26**	M5	55.31		SPECS SP	42.19	5.40
33	**S27**	M5	55.32		SPECS SP	4.39	0.55
34	**S28**	M6	57.59		In-house	0.83	0.11
35	**S29**	M6	57.48		SPECS SP	4.39	0.55
36	**54**	M6	57.13		In-house	51.31	2.02
37	**S30**	M6	57.10		In-house	8.29	4.07
38	**63**	M6	57.05		SPECS SP	71.15	5.38
39	**S31**	M6	57.04		SPECS SP	36.24	5.42
40	**53**	M6	56.51		SPECS NP	56.51	1.96
41	**S32**	M6	56.42		In-house	48.16	2.35
42	**S33**	Catalyst	-		In-house	41.38	1.74
43	**57**	Catalyst	-		In-house	64.42	10.3
44	**58**	Catalyst	-	M4	In-house	62.13	0.76
45	**59**	Catalyst	-		In-house	63.36	11.1
46	**S34**	Catalyst	-		In-house	3.06	1.12
47	**S35**	Catalyst	-		SPECS NP	19.74	2.91
48	**S36**	Catalyst	-		In-house	2.44	0.39
49	**S37**	Catalyst	-	M4	In-house	6.22	0.14
50	**61**	Catalyst	-	M4	In-house	78.88	8.97

[a]Predicted hit selected for biological screening to validate this specific model (compounds were selected to cover all pharmacophore models developed in this study). [b]Fit-score generated with the "pharmacophore-fit" scoring function in LigandScout. It is a quantitative metric that indicates how well the chemical functions of the ligand geometrically map the features of the pharmacophore model. [c]Some compounds are consensus hits of different models. This column describes the overlapping of positive hits. [d]Source from where the compound was obtained. [e]Percentage of peak tail hERG current reduction obtained at a compound's concentration of 30 µM in the oocyte assay ($n \geq 3$). hERG inhibition classification is color-coded: red – inactive (inhibition < 30%); light green – active with inhibition between 30 and 50%; dark green – active with inhibition ≥ 50% (compounds selected for IC_{50} determination).

Detailed workflow on the pharmacophores development.

M1. For pharmacophore generation the structures **4** and **40** were used. Prior to the pharmacophore generation the conformations for these 2 structures were calculated using the standard BEST configuration in the Ligand based view of LigandScout. Afterwards the shared feature

pharmacophores were generated and the first solution was selected. It included 3 hydrophobic features (HPFs), one hydrogen bond acceptor (HBA) and one positive ionizable feature (PIF) (tolerance size of 1.5). An exclusion volume coat was generated after the pharmacophore was already built. The resulting exclusion volumes (EXVOLs) were refined in the following way: 5 EXVOLs on position (-6.17, -6.68, 7.25; -1.67, -5.18, 5.75; 5.83, 2.32, 2.75; 2.83, -0.68, 4.25; 1.33, -3.68, 1.25) were deleted or deactivated. The size of all remaining EXVOLs was increased to a tolerance of 1.65, except for (-10.67, -6.68, 5.75 and -7.67, -9.68, 4.25) that were kept at 1.5 tolerance, and (-4.67, -2.18, 7.25 and -1.67, 3.82, -4.75) that were set to tolerance of 1.35 and 1.050001 respectively.

M2. This pharmacophore was built using molecules **41** and **42** as templates. 25 conformations were generated for these structures with the FAST configuration. After the shared feature pharmacophore generation, the first solution was chosen, which consisted of 4 HPFs and 1 aromatic ring feature (AR). The size of the HPFs on (7.65, 0.09, -2.57) were increased to a tolerance of 1.65, while the sizes of the other features stayed at the standard tolerance of 1.5, or at 0.9 in the case of the AR. The EXVOLs were created simultaneously to the pharmacophore generation and were increased in size to a tolerance of 2.25.

M3. This model was built out of the molecules **43** and **44**. Again 25 conformations were generated. Afterwards, the pharmacophore was generated and the first solution was chosen. The pharmacophore featured 1 HBA, 2 hydrogen bond donors (HBDs), 2 HPFs, 2 AR and 1 PIF. The HBA and the AR at (4.68, 1.36 and 1.92) were deleted and both HBDs and the PIF were increased in size to 1.8. The exclusion volumes coat was calculated during the pharmacophore generation. The following EXVOLs were deactivated or deleted: -9.52, -3.98, 7.54; -5.02, -5.48, 9.04; -2.02, -8.48, 7.54; -2.02, 5.02, 1.54; 6.98, 2.02, 6.04; -0.52, -0.98, -4.46; 2.48, -5.48, -2.96; 6.98, -6.98, -2.96; 9.98, 3.52, 3.04; 5.48, 5.02, -2,96; 9.98, 2.02, -2.96. Other EXVOLs were decreased in size to a tolerance of 1.35: -3.52, -3.98, -2.96; 2.48, 5.02, 0.04; -6.52, -0-98, -1.46; 9.98, -3.98, -1,46; 8.48, -3.98, -5.96; 2.48, 0.52, 7.54. Additionally two EXVOLS at positions -8.02, 0.52, 7.54 and 5.48, -2.48, 4.54 were decreased in size to a tolerance of 1.0500001.

M4. Structures **45** and **46** were used as templates. Conformations were calculated with the "FAST" configuration in the Ligand–based view of LigandScout. The first solution was chosen. The model comprises 2 HPFs, 1 AR, 1 HBA and 1 PI feature and none was deleted. The size of the two HPFs and the HBA was increased to 1.65. The EXVOLs were calculated simultaneously with the pharmacophore and some were deactivated: 2.64,4.87,-8.77; 1.14,-5.63,-8.77; 4.14, -2.63, -11.77; 2.64, -7.13, -4.27; 10.14, -4.13, -1.27; 8.64, 0.37, -2.77; 5.64, 4.87, -2.77; 5.64, -2.63, 0.23; -4.86, 0.37, 0.23; 7.14, -7.13, -4.27. Additional EXVOLs were added manually based on the structure of inactive molecules: 3.04, 0.83, -14.19 with a tolerance of 0.95000017; 0.32, 5.64, -13.20 with a tolerance of 1.7; -5.49, 4.11, -12.40 with a tolerance of 1.54; -5.73, 0.21, -14.09 with a tolerance of 1.4000001; -3.19, 1.83, -16.49 with a tolerance of 1.7; -2.66, -0.45, -15.68 with a tolerance of 1.54.

M5. Constructed out of molecules **47** and **48** (25 conformations calculated with the "FAST" configuration in the Ligand-based view). The seventh solution consisted of 3 HPFs, 1 HBA and 1 PIF, was chosen for further improvement. The tolerance of the two HPFs on positions 2.83, 18.91, 5.15 and 0.56, 22.19, 8.27 was increased to 1.65, and the tolerance of the HBA was increased to a value of 1.80. The exclusion volumes coat was generated with the 7 active hits from the highly

active database. All EXVOLs were increased in size to a tolerance of 2.7000003, except for 4.95, 11.69, 9.16 (feature size of 2.4), and 0.45, 13.19, -1.34 (feature size of 2.5500002).

M6. A different approach was employed for this model. Structures **49** with 109 conformations and **50** with 54 conformations were used for model generation. The eighth solution offered consisted of 6 features (2 HPFs, 1 PIF, 1 AR, 1 HBD and 1 HBA). The HBD was deleted and the remaining features were modified as described: the size of the two HPFs was decreased. The tolerance of the first HPF at position -2.31, -5.09, -0.26 was decreased to 1.35, while the tolerance of the second feature at position -4.62, 1.64, 3.54 was decreased to 1.2. The size of the PI and the HBA were also decreased to a tolerance of 1.35. The EXVOLs were calculated simultaneously, and three EXVOLs on positions -6.30, 0.65, 8.79; -7.07, -8.40, -1.20 and 2.84, -4.44, -3.97 were deleted. The size of two EXVOLs on positions -10.01, -0.81, 3.19 and -10.18, 1.27, 7.18 was decreased to a tolerance of 1.2.

Chemical property space analysis of known and new hERG blockers.

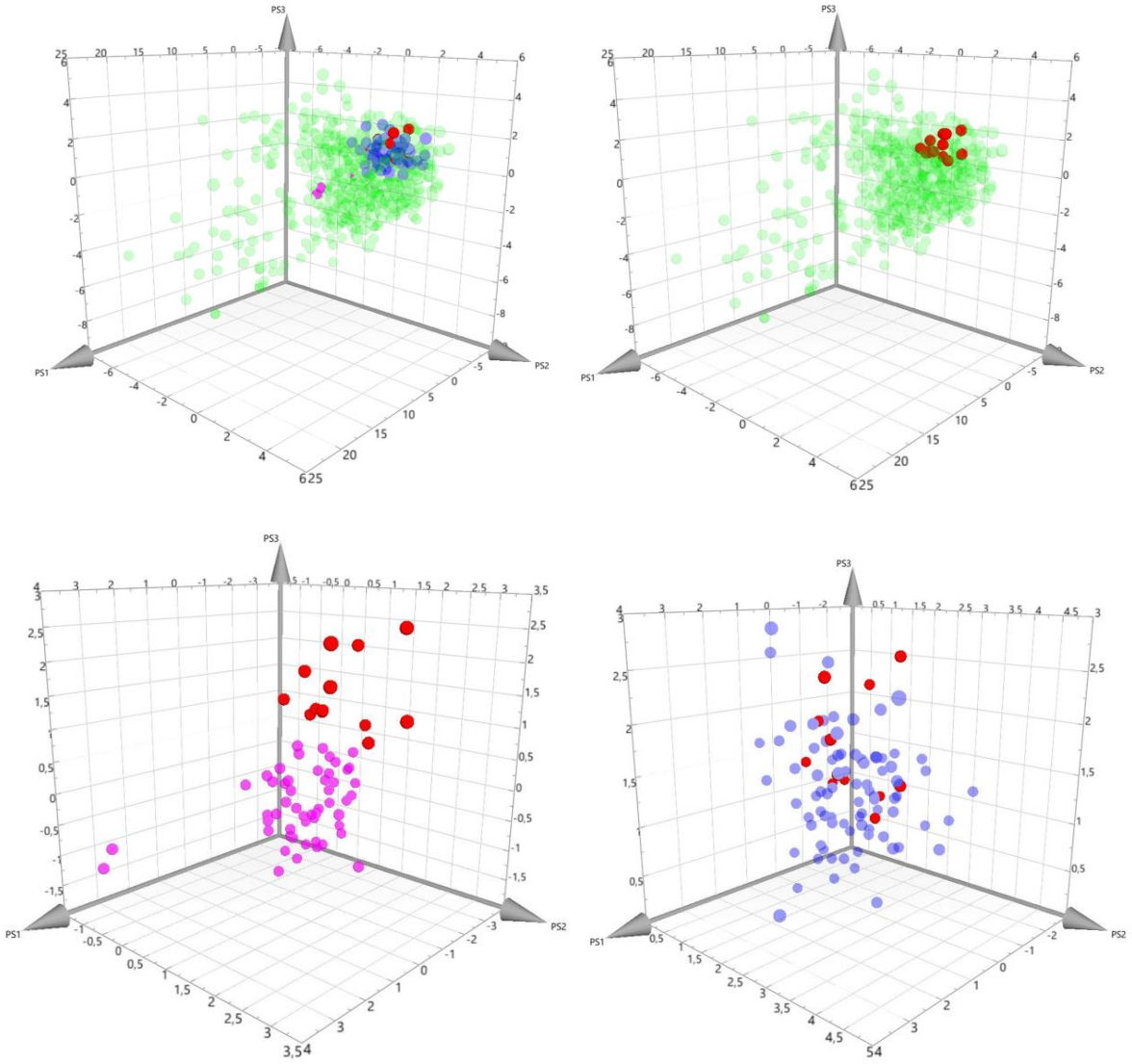

Figure S1. Analysis of the drug space coverage by the new hERG blockers identified in this study. The top left scatter plot depicts the 13 novel hERG blockers (red), together with three reference sets: FDA approved drugs (green – DrugBank, http://www.drugbank.ca/), highly active hERG blockers (IC_{50} < 1 µM) retrieved from ChEMBL and used as training set for LigandScout models (blue) and the de Bruin dataset[2] (purple). The other plots show individual comparison of datasets. The positions are determined by the three principal components from ChemGPS[3] (PS1: size, PS2: aromaticity, PS3: lipophilicity), which are summarized from a large number of molecular descriptors. The resulting cluster pattern can give valuable information on the structural diversity and biological properties of the compounds.

Full synthesis procedures of some of the compounds that were selected for biological evaluation.

Melting points were determined on a Kofler hot-stage microscope (Reichert) and are uncorrected. The IR spectra were taken on a Mattson Galaxy Series FT-IR 3000 spectrophotometer. The ^{1}H-NMR spectra were recorded on a Varian Gemini 200 spectrometer (199.98 MHz). The centre of the solvent multiplet was used as an internal standard, which was related to TMS with δ 7.26 ppm ($CDCl_3$) and 2.49 ppm (DMSO-d_6), respectively. Reactions were monitored by TLC using Polygram® SIL G/UV_{254} (Macherey-Nagel) plastic-backed plates (0.25 mm layer thickness) and visualized using an UV lamp. Elemental analyses were carried out at the Institute of Physical Chemistry (Mag. J. Theiner), University of Vienna, Austria.

Compound **62** (3-Chloro-6-{5-[1-(4-fluorophenyl)-piperazinyl]-pentyl}-8-methoxy-pyridazino[3,4-*b*][1,5]benzoxazepin-5(6*H*)-one).

A mixture of 0.430g (1 equivalent) of 3-chloro-6-(5-chloropentyl)-8-methoxypyridazino[3,4-*b*][1,5]benzoxazepin-5(6*H*)-one, 2 equivalents of 1-(4-fluorophenyl)-piperazine and 1 equivalent of sodium iodide in 25 mL of dry *N*,*N*-dimethyl formamide was stirred at 80 °C until the starting material was completely consumed (TLC monitoring, ethyl acetate, ca. 66 h). Then the mixture was poured into cold 1 *N* NaOH (70 mL) and the resulting mixture was extracted with ethyl acetate. The organic phase was washed with water and brine, dried over anhydrous sodium sulphate and evaporated. Purification by column chromatography (ethyl acetate) and subsequent recrystallization from a mixture of dichloromethane, diisopropyl ether and diethyl ether led to 21 % of yellow crystals. Mp 95-98 °C, IR (KBr) 1653 cm^{-1}; ^{1}H-NMR ($CDCl_3$) δ 7.95 (s, 1 H, H-4), 7.44 (d, J=8.8 Hz, 1H, phenyl-H), 6.99-6.74 (m, 6H, phenyl-H), 4.12 (t, J=7.1 Hz, 2H, CH_2), 3.80 (s, 3H, OCH_3), 3.13-3.08 (m, 4H, piperazinyl-CH_2), 2.58 (t, J=5.0 Hz, 4H, piperazinyl-CH_2), 2.38 (t, J=7.4 Hz, 2H, CH_2), 1.83-1.68 (m, 2H, CH_2), 1.62-1.34 (m, 4H, 2 x CH_2). Anal. $C_{27}H_{29}ClFN_5O_3$ (526.00). Calculated: %C 61.65, %H 5.56, %N 13.31. Found: %C 61.85, %H 5.46, %N 13.27.

Compound **S3** (6-[[[Bis(4-fluorophenyl)-methylene]amino]oxy]-hexanoic acid ethyl ester).

Preparation of the compound has already been described.[4] Yield: 80 %, IR (KBr) 1733 cm^{-1}; ^{1}H-NMR ($CDCl_3$) δ 7.49-7.29 (m, 4H, phenyl-H), 7.16-6.95 (m, 4H, phenyl-H), 4.20-4.06 (m, 4H, OCH_2, $COOCH_2CH_3$), 2.29 (t, J = 7.5 Hz, 2H, CH_2COOEt), 1.79-1.58 (m, 4H, 2xCH_2), 1.45-1.33 (m, 2H, CH_2), 1.24 (t, J = 7.2 Hz, 3H, CH_3). Anal. $C_{21}H_{23}F_2NO_3$ (375.42). Calculated: %C 67.19, %H 6.18, %N 3.73. Found: %C 66.95, %H 6.18, %N 3.71.

Compound **S4** (6,7-Dichloro-3-ethoxycarbonylmethyl-1-[(5'-trifluoromethylbenzothiazol-2'-yl)methyl]-quinoxalin-2(1*H*)-one and 6,7-Dichloro-3-ethoxycarbonylmethyliden-1-[(5'-trifluoro-methylbenzothiazol-2'-yl)methyl]-3,4-dihydrochinoxalin-2(1*H*)-one) (tautomeric forms).

The *N*(1*)*-benzothiazolylmethyl substituted quinoxalin-2(1*H*)-one was prepared in analogy to a known procedure:[5] A suspension of 1 mmol of 6,7-dichloro-1-cyanomethyl-3-ethoxycarbonyl-methylquinoxalin-2(1*H*)-one and equimolar amounts of 2-amino-4-trifluoromethylthiophenol hydrochloride in 10 mL dry ethanol was refluxed under nitrogen until TLC (eluent: dichloro-methane/ethyl acetate = 9/1) indicated no further conversion (8 days). After cooling to room

temperature, water was added and the resulting mixture was extracted with dichloromethane. The organic phase was washed with water and brine, dried over anhydrous sodium sulphate and evaporated. Purification was performed by two-fold column chromatography (first: dichloromethane/ethyl acetate = 9/1, second: dichloromethane/ethyl acetate = 50/1) and subsequent recrystallization from diisopropyl ether to give analytically pure compound in 9% as yellow crystals. Mp 213-215°C, IR (KBr) 1720, 1653, 1630 cm^{-1}. ^{1}H-NMR ($CDCl_3$) δ 11.20 (bs, '1.5 H', NH), 8.31-7.11 (m, '7.5H', aromatic H, both tautomers), 5.98 (s, 1H, =CH-COOEt, tautomer B), 5.79 (s, 1H, N-CH_2, tautomer A), 5.69 (s, 2H, N-CH_2, tautomer B), 4.25 (q, J=7.2 Hz, 3H, O-CH_2, both tautomers), 4.00 (s, 1H, CH_2-COOEt, tautomer A), 1.37-1.25 (m, '4.5 H', CH_3, both tautomers). The ratio of tautomers A:B is about 1:2. Anal. $C_{21}H_{14}Cl_2F_3N_3O_3S$ (516.33). Calculated: %C 48.85, %H 2.73, %N 8.14. Found: %C 48.73, %H 2.67, %N 8.05.

Compound **S5** (3-[3,4-Di-(4-bromo-2-fluorobenzyloxy)phenyl]-propionic acid).

Prepared from the appropriate ethyl ester derivative using a procedure described previously.[6] Recrystallization from ethyl acetate+diisopropyl ether led to 86 % of colourless crystals. Mp 141-144 °C, IR (KBr) 1714 cm^{-1}; ^{1}H-NMR (DMSO-d_6) δ 7.60-7.42 (m, 6H, phenyl H-3'/H-5'/H-6', phenyl H-3"/H-5"/H-6"), 7.01 (d, J_{26}=1.4 Hz, 1H, phenyl H-2), 6.97 (d, J_{56}=8.4 Hz, 1H, phenyl H-5), 6.77 ("d", J_{56}=8.4 Hz, 1H, phenyl H-6), 5.09 (s, 2H, CH_2), 5.06 (s, 2H, CH_2), 2.75 (t, J=7.7 Hz, 2H, $CH_2C\mathbf{H_2}CO$), 2.53-2.46 ("m", 2H, $C\mathbf{H_2}CH_2CO$). Anal. $C_{23}H_{18}Br_2F_2O_4$ (556.21). Calculated: %C 49.67, %H 3.26. Found: %C 49.63, %H 3.33.

Compound **S12** (2-(4-(4-Fluorophenylsulfonyl)piperazin-1-yl)pyrimidine).

127 mg of 2-(piperazin-1-yl)pyrimidine and 150 mg of 4-fluorobenzenesulfonyl chloride (1 equivalent) were dissolved in dichloromethane and heated in a CEM Discover microwave to 100°C for 10 minutes (250 Watt, 10 bars, closed vessel). The mixture was diluted with dichloromethane and washed twice with water. The organic layer was then washed with brine, dried over sodium sulphate, filtered and concentrated in vacuum. The crude product was purified by column chromatography (dichloromethane / 12.5% methanol), resulting in 225 mg of pure white solid (yield 90 %). ^{1}H-NMR (DMSO-d_6). δ = 2.90-3.05 (m, 4H, piperazinyl-CH_2), 3.72-3.94 (m, 4H, piperazinyl-CH_2), 6.64 (t, J = 4.7 Hz, 1H, pyrimidine-H5), 7.38-7.58 (m, 2H, phenyl-H), 7.73-7.93 (m, 2H, phenyl-H), 8.34 (d, J = 4.7 Hz, 2H, pyrimidine-H4/6).

Compound **S24** (DL-3-(5-trifluoromethylbenzothiazol-2-yloxy)-O-(5-trifluoromethylbenzothiazol-2-yl)-tyrosine methyl ester).

Prepared from equimolar amounts of DL-3-hydroxytyrosine methyl ester and 2-chloro-(5-trifluoromethylbenzothiazole using a procedure described previously.[7] Purification by column chromatography (ethyl acetate) and subsequent recrystallization from a mixture diisopropyl ether and diethyl ether led to pure compound (10% of yellow crystals). Mp 89-93°C, IR (KBr) 3346, 1743 cm^{-1}; ^{1}H-NMR (DMSO-d_6) δ 8.15-8.09 (m, 2H, phenyl-H), 7.81-7.56 (m, 6H, phenyl-H), 7.41-7.36 (m, 1H, phenyl-H), 3.70-3.63 (m, 4H, CH, CH_3), 3.07-2.81 (m, 2H, CH_2). Anal. $C_{26}H_{17}F_6N_3O_4S_2 \times 0.3$ DIPE (644.21). Calculated: %C 51.83, %H 3.32, %N 6.52. Found: %C 51.66, %H 3.12, %N 6.33.

Compound **S33** was prepared as described in reference [8].

Compound **S36** (2-Benzyl-4-(1-benzyl-5-chloropyrazol-3-yl)[1,2,4]triazolo[4,3-*a*]quinoxalin-1(2*H*)-one).

1.1 Equivalents of potassium *tert*-butanolate (0.129 g, 1.15 mmol) were added to 0.300 g (1.05 mol; 1 equivalent) of 4-(3(5)-chloro-1*H*-pyrazol-5(3)-yl)-[1,2,4]triazolo[4,3-*a*]quinoxalin-1(2*H*)-one in 30 mL of dry *N*,*N*-dimethyl formamide and the resulting mixture was stirred for one hour at 60°C. 1.1 equivalents of benzylbromide (0.197 g) were added and the reaction mixture was stirred at 110°C until TLC indicated no further conversion (some drops of the reaction mixture were treated with diluted HCl and extracted with ethyl acetate; TLC with diethyl ether as the mobile phase). Then, the mixture was poured into a mixture of 200 mL H_2O and 5 mL 2*N* HCl and the precipitate formed was filtered off, washed with water and dried in vacuum at 50°C. The raw product was purified by treatment of the solution with charcoal, followed by circular chromatography using dichloromethane/ethyl acetate (4/1) as eluting solvent, and final recrystallization from a mixture of ethyl acetate and diisopropyl ether to yield 24% of light pink crystals. Mp 170 °C, IR (KBr) 1720 cm^{-1}; ^{1}H-NMR ($CDCl_3$) δ 8.87 (dd, J=8.2 Hz, J=1.4 Hz, 1H, heteroaryl H), 7.83 (dd, J=7.9 Hz, J=1.7 Hz, 1H, heteroaryl H), 7.64 – 7.18 (m, 13 H, heteroaryl H, phenyl-H, pyrazolyl-H4), 6.04 (s, 2H, CH_2), 5.24 (s, 2H, CH_2). Anal. $C_{26}H_{19}ClN_6O \times 0.3$ ethyl acetate (493.36). Calculated: %C 66.22, %H 4.37, %N 17.03. Found: %C 66.13, %H 4.47, %N 17.05.

Compound **S37** (4-(1-Methyl-1*H*-pyrrol-2-yl)-1-(4-phenylpiperazin-1-yl-methyl)-[1,2,4]triazolo[4,3-*a*]quinoxaline).

For the synthesis, a mixture of 0.2 mmol (1 equivalent) of 1-chloromethyl-4-(1-methyl-1*H*-pyrrol-2-yl)-[1,2,4]triazolo[4,3-*a*]quinoxaline, 1 equivalent of *N*-phenylpiperazine, 2 equivalents of sodium carbonate, and 1 equivalent of potassium iodide in 5 mL of dry *N*,*N*-dimethyl formamide was stirred at 80°C until the starting material was completely consumed (TLC monitoring, dichloromethane/ethyl acetate (4/1), ca. 2.5 h). After cooling to room temperature, water was added and the resulting mixture was extracted with diethyl ether. The organic phase was washed with water and brine, dried over anhydrous sodium sulphate and evaporated to yield 0.075 g (90%) of the raw product. Recrystallization from ethanol led to the yellow orange crystals pure compound in 50% yield. Mp 213-215 °C, IR no characteristic peak, ^{1}H-NMR ($CDCl_3$) δ 8.53 - 8.45 (m, 1 H), 8.03 - 7.97 (m, 1 H), 7.63 - 7.49 (m, 2 H), 7.29 - 7.19 (m, 2 H), 6.96 - 6.81 (m, 4 H) (quinoxaline-H, phenyl-H, pyrrolyl-H5), 8.18 (dd, J_{35} = 1.6 Hz, J_{34} = 4.1 Hz, 1 H, pyrrolyl-H3), 6.34 (dd, J_{43} = 4.1 Hz, J_{45} = 2.6 Hz, 1 H, pyrrolyl-H4), 4.33 (s, 2 H, CH_2), 4.24 (s, 3 H, *N*-CH_3), 3.23 - 3.18 (m, 4 H), 2.86 - 2.81 (m, 4 H) (piperazinyl-CH_2). Anal. $C_{25}H_{25}N_7$ (423.52). Calculated: %C 70.90, %H 5.95, %N 23.15. Found: %C 70.69, %H 5.65, %N 22.99.

Compound **61** was prepared as previously described.[9]

Supporting Information References

1. Ekins, S.; Crumb, W. J.; Sarazan, R. D.; Wikel, J. H.; Wrighton, S. A. Three-dimensional quantitative structure-activity relationship for inhibition of human ether-a-go-go-related gene potassium channel. *J. Pharmacol. Exp. Ther*. **2002**, 301, 427-434.

2. de Bruin, M. L.; Pettersson, M.; Meyboon, R. H. B.; Hoes, A. W.; Leufkens, H. G. M. Anti-HERG activity and the risk of drug-induced arrhythmias and sudden death. *Eur. Heart J.* **2005**, 26, 590-597.

3. Oprea, T. I.; Gottfries, J. Chemography: the art of navigating in chemical space. *J. Comb. Chem.* **2001**, 3, 157-166.

4. Rakowitz, D.; Piccolruaz, G.; Pirker, C.; Matuszczak, B. Novel Aldose Reductase Inhibitors Derived from 6-[[(Diphenylmethylene)amino]oxy]hexanoic Acid. *Arch. Pharm. Pharm. Med. Chem.* **2007**, 340, 202-208.

5. Aotsuka, T.; Hosono, H.; Kurihara, T.; Nakamura, Y.; Matsui, T.; Kobayashi, F. Novel and Potent Aldose Reductase Inhibitors: 4-Benzyl- and 4-(Benzothiazol-2-ylmethyl)-3,4-dihydro-3-oxo-2H-1,4-benzothiazine-2-acetic Acid Derivatives. *Chem. Pharm. Bull*. **1994**, 42, 1264-1271.

6. Rakowitz, D.; Gmeiner, A.; Schröder, N.; Matuszczak, B. Synthesis of novel phenylacetic acid derivatives with halogenated benzyl subunit and evaluation as aldose reductase inhibitors. *Eur J. Pharm. Sci*. **2006**, 27, 188–193.

7. a) Rakowitz, D.; Hennig, B.; Nagano, M.; Steger, S.; Costantino, L.; Matuszczak, B. Synthesis of novel benzoic acid derivatives with benzothiazolyl subunit and evaluation as aldose reductase inhibitors', *Arch. Pharm. Pharm. Med. Chem.* **2005**, 338, 411-418. b) Rakowitz, D.; Muigg, P.; Schröder, N.; Matuszczak, B. On the synthesis of bioisosters of O-benzothiazolyloxybenzoic acids and evaluation as aldose reductase inhibitors, *Arch. Pharm. Pharm. Med. Chem.* **2005**, 338, 419-426.

8. Ott, I.; Kircher, B.; Heinisch, G.; Matuszczak, B. Substituted pyridazino[3,4-*b*][1,5]benzoxazepin-5(6*H*)ones as multidrug-resistance modulating agents. *J. Med. Chem.* **2004**, 47, 4627-4630.

9. Matuszczak, B.; Mereiter, K. Syntheses in the series of pyrazolyl-substituted quinoxalines. *Heterocycles* **1997**, 45, 2449-2462.